Archives of Environmental Protection
Vol. 52 no. 2 pp. 105–117

PL ISSN 2083-4772
DOI: 10.24425/aep.2026.1297

Changes in the concentration levels of polycyclic aromatic hydrocarbons in the soil – a case study of a city in southern Poland

Wojciech Rykała*[1], Dominika Dąbrowska[1], Monika J. Fabiańska[1], Barbara Szaflik[1],Youssef M. Youssef[2]

[1]Faculty of Natural Sciences, University of Silesia, Sosnowiec: Poland
[2]Geological and Geophysical Engineering Department, Faculty of Petroleum and Mining Engineering, Suez University, Suez, Egypt

*Corresponding author's e-mails: wojciech.rykala@us.edu.pl

Keywords: organic compounds, contamination, gas chromatography-mass spectrometry, diagnostic ratios.

Abstract: Polycyclic aromatic hydrocarbons (PAHs) are organic compounds considered carcinogenic, teratogenic and mutagenic, and they can migrate into soil and water environments. The aim of this article is to present potential changes in PAH concentrations in the tested soil samples from the city of Będzin, located in southern Poland, across two measurement series, and to identify potential sources of contamination. Thirty soil samples were collected in two measurement series. Sample locations associated with high traffic intensity and power plants showed higher average concentrations of PAHs in late spring. In contrast, locations associated with high population density showed higher concentrations in late autumn. The average concentration of the analyzed PAHs (PAHsum) in 15 soil samples from the first sampling (A) was 151 µg/g, while from the second sampling (B) it was 246 µg/g. The values of the ΣPAHcarc/ΣPAH toxicity index in all tested soil samples remained below 0.4. The current level of soil contamination in this region indicates greater accumulation of PAHs from former industrial plants than from current ones. Despite this fact, continuous monitoring of these compounds is important to prevent the migration of contaminants into aquifers.

Introduction

Polycyclic aromatic hydrocarbons (PAHs) are organic compounds consisting of multiple fused benzene rings and are commonly detected in various environmental compartments (Ncube et al. 2018). These compounds are recognized for their carcinogenic, teratogenic, and mutagenic properties (Rykała et al. 2023). PAHs tend to accumulate in soil and water environments, with industrialization identified as the primary factor contributing to their presence (Abdel-Shafy and Mansourm 2016). They are mainly produced through the incomplete combustion of fossil fuels, biomass, and biofuels; however, other processes, such as fires and waste treatment, also contribute to their formation and subsequent atmospheric emission (Almouallem et al. 2023).

Structurally, PAHs containing one to six aromatic rings are categorized as "small," while those with seven or more rings are considered "large" (Sun et al. 2021). Based on their origin, PAHs can be classified into three groups, i.e., pyrogenic, petrogenic and biological (Mojiri et al. 2019). Due to their widespread presence in sediments, sewage, and fuels, PAHs readily migrate into surface water, soil, and groundwater systems (Gutierrez-Urbano et al. 2021). In biological systems, PAHs bioaccumulate in tissues such as the liver, adipose tissue, lungs, kidneys, skin, and placenta (Ramesh et al. 2004), potentially causing damage to the circulatory, nervous, and reproductive systems. Their toxicity increases with molecular size, and carcinogenesis is initiated through interactions with DNA, RNA, and proteins. PAHs containing more than four benzene rings are considered the most biologically active. Among them, benzo(a)pyrene exhibits the highest carcinogenicity, and a relationship has been identified between its concentration in the air and the incidence of lung cancer (Bukowska et al. 2022). Due to their lipophilic properties (i.e., affinity for lipids), aromatic hydrocarbons and their derivatives preferentially accumulate in the fatty tissues of mammals (Wilcke et al. 2014).

In recent years, numerous studies have focused on PAH contamination in urban soils worldwide. Vance et al. (2014) analyzed 76 locations across London (UK), reporting concentrations of 16 parent compounds ranging from 4–67 mg/kg (average 18 mg/kg) and total PAHs (33 compounds) ranging from 6 to 88 mg/kg. Fluoranthene and pyrene were the most abundant compounds, and the predominance of four- to six-ring PAHs indicated sources such as coal, oil combustion, and traffic emissions. Their spatial distribution also suggested weathering processes, including volatilization and biodegradation.

Shamilishvily et al. (2018) investigated PAH composition in urban soils from parks, residential areas and industrial zones in St. Petersburg, Russia. Similarly, Liu et al. (2024) examined urban soils under different terrain conditions in Taiyuan, China. (Paradelo et al. (2023) studied contaminated soils in Santiago de Compostela, Spain. Lehndorff et al. (2004) identified a link between PAH concentrations and $PM_{2.5}$ emissions in Cologne, with phenanthrene, fluoranthene, and pyrene as predominant compounds. In the United States, PAH concentrations in soils have been shown to correlate with urban development, population density, and emission sources (Lopes et al. 1998).

In Poland, coal mining remains a key industrial sector, with the country ranking second in Europe and ninth globally in coal production. Nearly all extracted coal is consumed domestically for electricity generation and heating. As a result, PAH levels in soils are regularly monitored by the State Environmental Monitoring program in accordance with national regulations (Journal of Laws 2024, item 54). The city of Będzin, located in southern Poland, is one of the oldest towns in the Upper Silesian Coal Basin and an important center of heavy industry and mining, with a high population density of 1,452 persons/ km^2.

Despite Będzin's industrial importance, most existing research has focused on PAH levels in agricultural or industrials soils. For instance, Maliszewska-Kordybach et al. (2008) reported that agricultural soils contain Σ16 PAHs ranging from 80 to 7264 µg/kg (average 395 µg/kg), predominantly four- to six-ring compounds. Higher concentrations are typically observed in industrial cities. Recent assessments by the Polish Geological Institute also confirm that Będzin's environment is heavily impacted by mining activities. However, a significant knowledge gap remains regarding PAH contamination in urban riverine soils affected by mining and industrial operations in Będzin.

Thus, this study focuses on the eastern part of Będzin to investigate sources of soil contamination across different seasons. The main aim is to assess changes in PAH concentrations in the tested soil samples collected from the city of Będzin across two measurement series and to identify potential sources of contamination. The findings are expected to provide valuable insights for environmental protection and contamination management in urbanized riverine cities.

Materials & Methods

Study area

The research area covers Będzin, a city in southern Poland (Silesian Voivodeship, Będzin County) with an area of approximately 3,739 hectare (ha). It borders with the municipalities of Dąbrowa Górnicza, Sosnowiec, Czeladź, Siemianowice Śląskie, Wojkowice, and Psary, and is located near key transportation corridors, including major roadways and railway lines.

The topography of Będzin is characterized by low hills and flat-bottomed valleys, primarily shaped by the Przemsza River. Geologically, the region consists of Carboniferous rocks overlain by Triassic dolomites and limestones, which are characteristic of the structural relief of the Silesian Upland.

Based on an analysis of urban development, the predominant land use in Będzin the city comprises urbanized areas (approximately 42.7%), followed by agricultural land (approximately 36.5%), industrial zones (approximately 5.8%), transportation infrastructure (approximately 9.9%), and forested areas (approximately 5.1%). These land cover distributions were determined using data from the Corine Land Cover program. Within the city's administrative boundaries, the most extensive category is residential development, accounting for approximately 33.9% of the total area, followed by arable land (16.1%) and meadows and pastures (13.2%).

Sampling

Measuring points for field research were selected to show differences in the development of the city of Będzin. First, the sampling sites were analyzed using orthophotomaps, local spatial development plans, and materials from the General

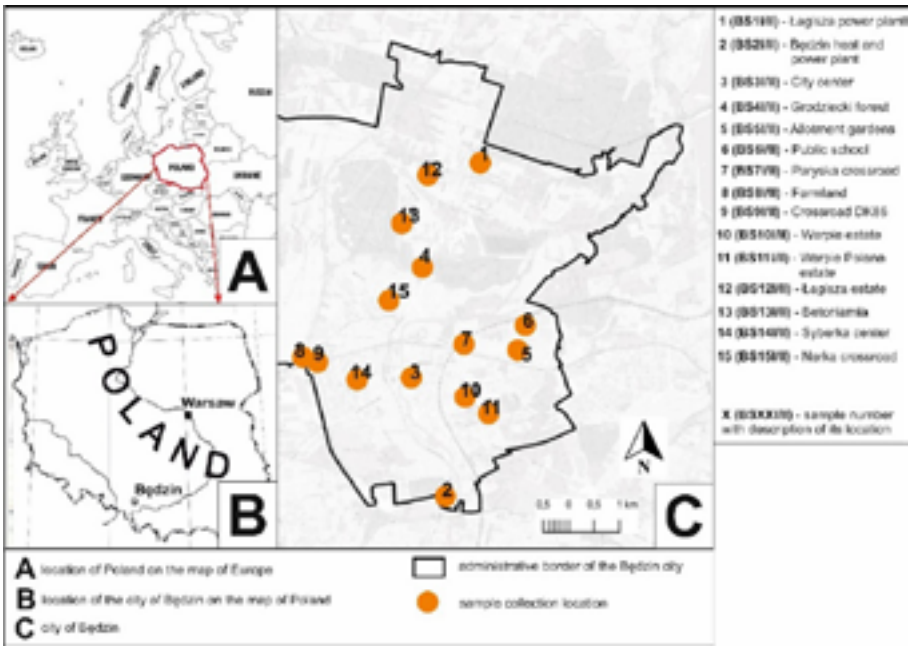

Fig. 1. Maps locations of the city of Będzin with sampling locations

Directorate for Environmental Protection, particularly with regard to historically polluted areas.

The selection of sampling locations in the study was based on prior analysis and interpretation of terrain characteristics and population density. Finally, 15 areas were selected for study. In addition, the locations were chosen to ensure diversity in research results due to the presence of different types of pollutant emitters. The study also considered two different seasons of the year to capture variability between them.

Fifteen locations were designated for soil sample collection at two-time intervals. The first set of 15 samples was collected in May (late spring) 2023 (BS1I-BS15I), while the second set, from the same locations, was collected in November (late autumn) 2023 (BS1II-BS15II). In total, 30 soil samples were collected. The characteristics of the sampling sites and their locations relative to the city boundaries are presented in Figure 1. Because PAHs are hydrophobic compounds that strongly sorb organic matter and accumulate mainly in the surface layer, samples were collected from a depth of up to 10 cm. Only soil was sampled, excluding the aboveground vegetation layer. Samples weighing approximately 20-30 g were collected using a steel spatula and placed into glass transport containers. The containers were then sealed and secured for safe transport to the laboratory at the Institute of Earth Sciences in Sosnowiec. In a controlled and sterile laboratory environment (constant ambient temperature, with no risk of contamination), the samples were air-dried at room temperature (approx. 21°C) for 4-5 days until completely dry. The dried soil samples were then labelled and manually crushed to a particle size fraction of <0.2 mm.

Solvent extraction

Soil samples (ca. 20 g) were extracted in an ultrasonic bath at 30°C for 15 min (3 times) using dichloromethane (DCM). The extracts were filtered through filter paper discs (grade 3 m/N; diameter 110 mm), after which the solvent was evaporated at room temperature and the extract yield was determined. Recovery values following filtration with 3 successive sample washings were approximately 75-87%. The obtained sample extracts were dissolved in 1.5 ml of ethyl acetate, and each sample was analyzed separately using gas chromatography-mass spectrometry (GC-MS).

Gas chromatography-mass spectrometry (GC-MS)

GC-MS analysis was performed at the Faculty of Natural Sciences in Sosnowiec, Poland, using an Agilent Technologies 7890A gas chromatograph coupled with an Agilent 5975C mass spectrometer equipped with a triple-axis detector. Helium (grade 6.0) was used as the carrier gas at a constant flow rate of 2.6 ml/min. The GC oven temperature program was as follows: initial temperature of 45°C (held for 1 min), increased to 100°C at 20°C/min, and then to 300°C (held for 60 min) at 3°C/min. The solvent delay was set to 10 min. The injector temperature was maintained at 200°C. Separation was achieved using a J&W HP-5MS fused silica capillary column (60 m x 0.32 mm i.d., 0.25 µm film thickness) coated with a chemically bonded stationary phase (5% phenyl, 95% methylsiloxane). Mass spectra were acquired in electron ionization (EI) mode at 70 eV over the mass range of 45–550 Da (0–40 min) and 50–700 Da (>40 min). Compounds were identified based on mass spectra, comparison of retention times with standard compounds, literature data, and interpretation of fragmentation patterns. Each sample was analyzed in triplicate.

Quality Assurance and Quality Control (QA/QC)

In order to evaluate potential contamination during the analytical process, a procedural blank encompassing the entire method was analyzed alongside each sample series as a part of quality assurance and quality control (QA/QC). Method performance was verified using the NIST SRM 1649b reference material by comparing the obtained results with certified concentrations of the target PAHs (Table 2). Limits of detection (LODs) were determined from three replicate procedural blanks as three times the standard deviation of the background signal. The average LOD values were 2.0 ± 0.05 ng/ml. Values below LOD were treated as zero for all calculations. Peaks were manually integrated. Quantitative analysis was based on 5-point calibration curves prepared from analytical standards. A linear relationship between peak area and PAH concentration was observed over the range of 0.10 and 10 µg/ml, with correlation coefficient values between 0.997 and 0.998. The mean extraction recoveries were of 71, 90, 93, and 85 for naphthalene, phenanthrene, benzo(a)pyrene, and perylene, respectively.

Calculations

The mutagenicity equivalent (MEQ) and carcinogenic equivalent (TEQ) are widely used metrics for estimating the total mutagenic and carcinogenic potential of a mixture of PAHs relative to a reference compound, typically benzo(a)pyrene (BaP) (Wang et al. 2023). These values are calculated by summing the concentrations of individual PAHs multiplied by their respective mutagenic potency factors (MEF) or toxicity equivalent factors (TEF). The resulting values are presented in Table 1.

Table 1: The potency factors of PAHs

PAH Compound	Abbreviation	Mutagenic Potency Factor (MEF) (Jung et al., 2010)	Toxicity Equivalent Factor (TEF) (Jung et al., 2010)
Benzo(a)anthracene	BaA	0.082	0.1
Chrysene	Ch	0.017	0.01
Benzo(b)fluoranthene	BbF	0.25	0.1
Benzo(k)fluoranthene	BkF	0.11	0.1
Benzo(a)pyrene	BaP	1.0	1.0
Indeno[1,2,3-cd]pyrene	IP	0.31	0.1
Dibenzo(a+h)anthracene	DB	0.29	5.0
Benzo(ghi)perylene	BghiP	0.19	0.01

The $\Sigma PAH_{carc}/\Sigma PAH$ toxicity index is a simplified metric that represents the proportion of carcinogenic PAHs within a total PAH mixture. It expresses the ratio of the mass of carcinogenic compounds to the total mass of all measured PAHs.

Defining threshold values is crucial for interpreting the results of risk assessments. There are no universally established regulatory thresholds for MEQ; therefore, values are interpreted in relation to the reference compound, benzo(a)pyrene BaP. For TEQ, several health organizations have established guideline values for BaP in ambient air, which serve as a proxy for the acceptable risk level of a PAH mixture. The European Union and the World Health Organization have set a reference value or target of 1.0 ng/m³ for the annual average concentration of BaP in ambient air. Therefore, a BaP-TEQ value exceeding 1.0 ng/m³ is generally considered indicative of potential health concern. The $\Sigma PAH_{carc}/\Sigma PAH$ index is interpreted based on its proximity to 1.0. A ratio well below 1.0 indicates that carcinogenic compounds constitute a small fraction of the total PAHs, suggesting low risk.

Hierarchical analysis

To identify natural groupings and similarities among the collected soil samples, hierarchical cluster analysis (HCA) was performed using the Python programming language. This analysis was based on calculated geochemical parameters, specifically the methylnaphthalene index (MNR), methylphenanthrene indices (MPI-1, MPI-3), and calculated vitrinite reflectance (R_c).Prior to clustering, the data were standardized using the StandardScaler function. Standardization is a preprocessing step in distance-based algorithms, whereby the mean is removed, and each feature is scaled to unit variance. As a result, all parameters contribute equally to the analysis, preventing features with larger numerical ranges from disproportionately influencing the clustering result. After standardization, each feature had a mean of 0 and a standard deviation of 1.

The hierarchical clustering method begins by treating each sample as a single cluster. In subsequent steps, the algorithm iteratively merges the two closest clusters into a larger cluster until all samples are combined into a single cluster. Ward's minimum variance method was used to determine the distance between clusters, merging at each step the pair that results in the minimal increase in the total within-cluster sum of squares. Distances between individual samples was calculated using the Euclidean metric. The final assignment of samples to a specified number of clusters was performed using the AgglomerativeClustering function. The primary parameter, n_clusters, defines the target number of clusters for the data.

Results & Discussions

PAHs analyses

A number of polycyclic aromatic hydrocarbons (PAHs) were detected in the tested samples (Table 2; Figure 2), including compounds containing two, three, four, five, and six rings.

The average concentration of the analyzed PAHs (PAH_{sum}) in 15 soil samples from the first sampling campaign (A) was 151.23 µg/g, whereas in the second sampling campaign (B) it was 246.25 µg/g. The samples were classified into 4 categories based on PAH_{sum} concentration: (i) low (<10 µg/g), (ii) moderate (10–100 µg/g), (iii) high (101–1000 µg/g), and (iv) very high (>1000 µg/g). Only 1 soil sample BS10II fell into the very high category (iv), while no samples were classified in the lowest category (i). of the elevated PAH concentration in sample BS10II may be attributed to several factors. Firstly, increased traffic in the area, which is residential in nature. Secondly, short-term contamination of the sampling site due to anthropogenic activities not detectable macroscopically (e.g., discharge of waste or sewage). Category (iii) included a similar number of soil samples from both sampling campaigns: 9 samples from the first campaign (BS1I-BS2I, BS6I-BS7I, BS9I-BS12I, BS15I) and 8 samples from the second sampling campaign (BS2II-BS4II, BS6II-BS7II, BS11II-BS13II). A comparable distribution was observed for category (ii), with 6 soil samples in each campaign: first campaign (BS3I-BS5I, BS8I, BS13I-BS14I) and second campaign (BS1II, BS5II, BS8II-BS9II, BS13II, BS15II).

Figure 3 shows the percentage distribution of 2-6 ring cyclic PAHs in the tested soil samples. The most dominant PAHs in both sampling campaigns were 4-ring compounds (Fl, Py, BaA, Ch) in both May and November samples. Py is mainly derived from the combustion of biomass and coal (Pokhrel et al. 2018, Yunker et al. 2002). The highest concentrations were recorded in the following samples: (A) - BS1I, BS10I, BS15I (148.42 µg/g, 136.61 µg/g, 140.54 µg/g, respectively); and (B) – BS3II, BS4II, BS10II (241.44 µg/g, 143.82 µg/g, 407.48 µg/g respectively). Three-ring PAHs (F, P, A, Ace, Acy) ranged from 17-53% in samples (A) and 27-50% in samples (B). Five-ring PAHs (BcPhe, Bb + kF, BaF, BaP, BeP, Pe) were detected in all

Table 2: Diagnostic ions of detected PAHs

PAHs	Short	m/z	PAHs	Short	m/z
Naphthalene	(N)	128	Chrysene	(Ch)	228
Acenaphthylene	(Acy)	152	Benzo(b+k)fluoranthene	(Bb+kF)	252
Acenaphthene	(Ace)	154	Benzo(a)fluoranthene	(BaF)	252
Fluorene	(F)	166	Benzo(a)pyrene	(BaP)	252
Phenanthrene	(P)	178	Benzo(e)pyrene	(BeP)	252
Anthracene	(A)	178	Perylene	(Pe)	252
Fluoranthene	(Fl)	202	Indeno[1,2,3-cd]pyrene	(IP)	276
Pyrene	(Py)	202	Benzo(ghi)perylene	(BghiP)	276
Benzo(c)phenanthrene	(BcPhe)	228	Dibenzo(a+h)anthracene	(DB)	278
Benzo(a)anthracene	(BaA)	228			

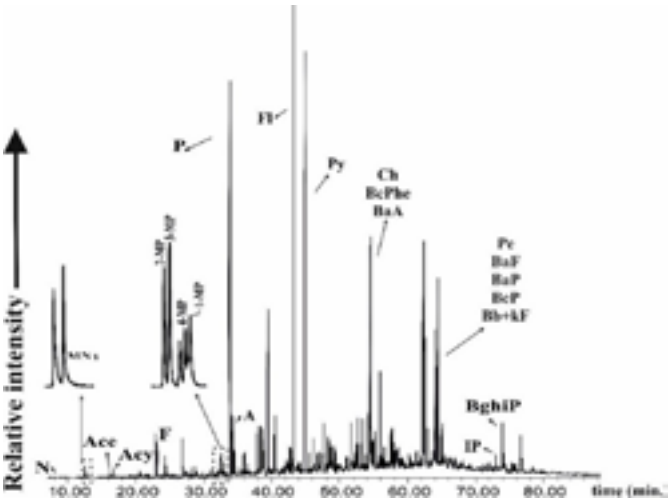

Fig. 2. Ion chromatograms of alkylnaphthalenes (m/z = 142), alkylphenanthrenes (m/z = 192), and generalized PAHs distribution

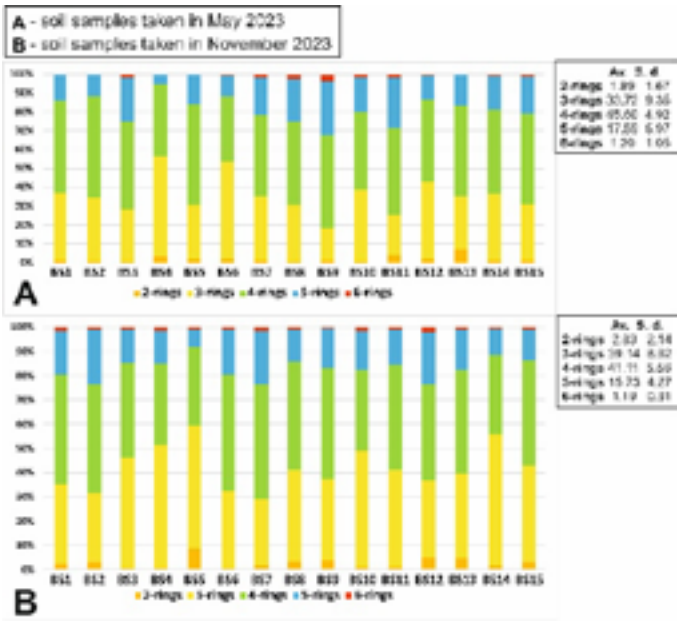

Fig. 3. Distribution pattern (%) of 2–6-ring PAHs in the soil samples

samples, with proportions ranging from 5 to 28% in samples (A) and 7 to 22% in samples (B). Dibenzo(a+h)anthracene (DB) was detected in small amounts or was not found in the tested samples. The heaviest 6-ring PAHs (IP, BghiP) were detected more often in autumn samples from November (15 occurrences; 0.9-1.9%) than in late spring samples from May (11 occurrences: 0.2-3.6%). High-molecular-weight PAHs (four or more rings) are generally considered to be produced mainly by combustion processes at high temperatures (Wang et al. 2006).

The MEQ mutagenicity equivalent (Błaszczyk et al. 2016) (Table 3) was, on average, slightly higher in late autumn soil samples (the range: 1.894-76.957; mean: 14.53). However, these values do not pose a risk to human health. The ΣPAH_{carc}/ΣPAH toxicity index in all tested soil samples remained below 0.363 (mean: 0.24), indicating a low risk to human health from carcinogenic PAHs, for which the maximum risk factor is 1. These values are also much lower compared to strongly contaminated environments (Rykała et al. 2024) and slightly lower than those observed in other cities in southern Poland (Rogula-Kozłowska et al. 2013). The TCDD-TEQ carcinogenicity equivalent also showed low values (0.01-0.29). These results may additionally confirm the accumulation of legacy pollution in soils, which can still be observed in urban areas associated with former mines or industrial plants in southern Poland (Kozielska and Rogula-Kozłowska 2014).

Geochemical ratios based on alkyl aromatic hydrocarbons in soil

Methylphenanthrenes (*m/z* = 192) and Methylnaphthalenes (*m/z* = 142) (Figure 4) were found in most of the tested soil samples. MNR values ranged from 0.97 to 3.65 in late spring samples and 1.20 to 2.57 in late autumn samples. MPI-1 and MPI-3 values (methylphenanthrene indices) varied as follows: for MPI-1, from 1.64 (BS11I) to 2.67 (BS6I) in May, and from 1.86 (BS8II) to 2.73 (BS4II) in November; for MPI-3, from 1.16 (BS5I) to 1.78 (BS6I) in May and from 1.24 (BS8II) to 1.94 (BS10II) in November (Table 4).

MPI-1 values were calculated using the fossil fuel vitrinite reflectance equation proposed by Radke (1988). These values were subsequently used to estimate the equivalent vitrinite reflectance (R_c), following the formula established by Radke et al. (1986). The elevated R_c values observed in the analyzed soil samples suggest that the organic matter has undergone significant thermal alteration. Samples collected during both sampling periods fall within the mixed-combustion range (Figure 4), indicating multiple sources of PAH contamination, such as emissions from motor vehicles and hard coal combustion (Fabiańska et al. 2017; Nádudvari and Fabiańska 2015). The observed variability in MPI-1 values is consistent with differences in combustion processes. Notably, slightly higher mean MPI-1 values were recorded in the samples collected in November.

Furthermore, the strong linear correlation between MPI-1 and MPI-3 suggests that the methylphenanthrenes present in the soil likely originate from a common source of contamination. Based on geochemical characteristics, it can be inferred that a portion of the emissions may be of petrogenic origin, likely associated with petroleum-derived pollutants.

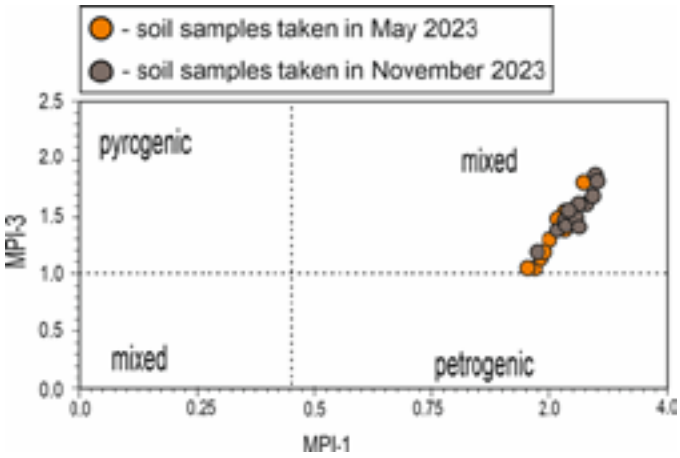

Fig. 4. Diagnostic diagrams of MPI-1 versus MPI-3

Table 3: Environmental toxicity indicators from collected soil samples (µg/g)

Sample code	PAH_{sum} µg/g	RTBaP	$\sum PAH_{carc}/\sum PAH$	MEQ	TCDD-TEQ	BaPE µg/g	Sample code	PAH_{sum} µg/g	RTBaP	$\sum PAH_{carc}/\sum PAH$	MEQ	TCDD-TEQ	BaPE µg/g
BS1I	302.35	10.871	0.228	14.106	0.07	9.14	BS1II	90.28	4.571	0.270	5.948	0.03	3.85
BS2I	149.38	4.912	0.209	6.167	0.03	4.03	BS2II	195.70	11.937	0.321	15.625	0.07	10.25
BS3I	69.35	4.431	0.301	5.790	0.02	3.81	BS3II	614.52	24.623	0.218	31.416	0.13	20.61
BS4I	98.91	1.600	0.104	1.941	0.01	1.28	BS4II	425.68	17.194	0.197	21.961	0.09	14.52
BS5I	31.69	1.349	0.239	1.721	0.01	1.16	BS5II	74.78	1.444	0.122	1.894	0.01	1.11
BS6I	274.36	8.454	0.167	10.993	0.05	6.99	BS6II	227.92	11.466	0.280	15.097	0.07	9.66
BS7I	125.57	7.042	0.262	9.080	0.04	6.03	BS7II	159.60	9.748	0.321	12.786	0.06	8.34
BS8I	76.06	4.928	0.289	6.356	0.03	4.24	BS8II	88.84	3.417	0.231	4.371	0.02	2.82
BS9I	131.05	10.869	0.363	14.063	0.05	9.33	BS9II	36.70	1.620	0.250	2.090	0.01	1.37
BS10I	330.22	16.998	0.245	21.975	0.09	14.48	BS10II	1233.46	61.537	0.215	76.957	0.29	52.81
BS11I	192.46	13.321	0.343	17.538	0.08	11.49	BS11II	151.45	6.350	0.232	8.097	0.03	5.31
BS12I	102.32	3.477	0.190	4.474	0.02	2.91	BS12II	111.92	6.746	0.293	8.789	0.04	5.78
BS13I	32.38	1.362	0.244	1.782	0.01	1.17	BS13II	75.09	3.475	0.262	4.504	0.02	2.93
BS14I	57.15	2.588	0.242	3.410	0.02	2.19	BS14II	154.44	4.612	0.167	5.863	0.03	3.77
BS15I	295.23	15.352	0.271	20.112	0.09	13.07	BS15II	53.39	1.964	0.224	2.517	0.01	1.61
V. r.	31.69-295.23	1.3-16.998	0.104-0.363	1.782-21.975	0.01-0.09	1.17-14.48	V. r.	36.7-1233.46	1.62-61.537	0.122-0.321	2.09-76.957	0.01-0.29	1.37-52.81
Av.	151.23	7.17	0.25	9.30	0.04	6.09	Av.	246.25	11.38	0.24	14.53	0.06	9.65
S. d.	102.92	5.22	0.07	6.82	0.03	4.46	S. d.	313.64	15.30	0.05	19.14	0.07	13.12

V. r. – Values range, Av. – Average values, S. d. - Standard deviation.

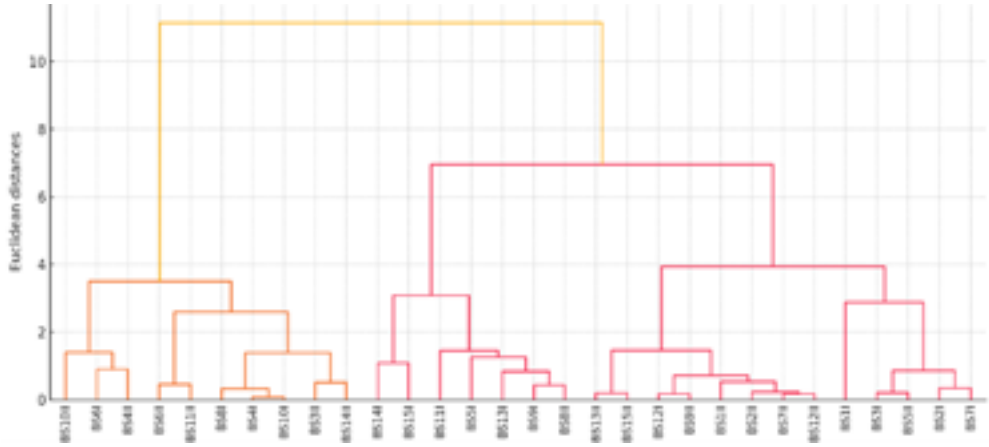

Fig. 5. Dendrogram for the analyzed samples

Cluster analysis was performed on the data presented in Table 4 using the Python programming language. The aim of the analysis was to examine the similarity among the collected samples based on the MNR, MPI-3, MPI-1, and R_c parameters. Prior to clustering, the data were standardized using the StandardScaler function to achieve a zero mean and a standard deviation of 1. Hierarchical agglomerative clustering was then conducted using Ward's method, which minimizes the increase in total within-cluster variance during cluster merging. Euclidean distance was used as the similarity metric between samples. The results of the analysis is presented in Figure 5.

Based on the presented graph, four clusters were selected, and samples were assigned to them according to data similarity. The Agglomerative Clustering function was used to ensure unambiguous assignment.

The first cluster contains the following samples: BS4I, BS6I, BS8I, BS10I, BS3II, BS4II, BS6II, BS10II, BS11II, BS14II, The second includes BS1I, BS2I, BS3I, BS7I. The third cluster comprises BS5I, BS9I, BS11I, BS13I, BS14I, and BS15I, while the fourth cluster consists of BS12I, BS1II, BS2II, BS7II, BS9II, BS12II, BS13II, BS15II. The first cluster is characterized by the highest mean values of the MPI-1 and R_c features. The second cluster exhibits the lowest MPI-3 values. The third cluster shows the lowest mean values across all features except MPI-3, whereas the fourth cluster is distinguished by the lowest standard deviations and balanced feature values.

When the obtained results are related to location, it can be observed that the first cluster includes samples from urban areas situated slightly away from main roads or with a partial presence of greenery. The second cluster comprises areas negatively affected by industrial environments or exposed to long-term urban impact. The third cluster is dominated by residential areas with access to greenery or characterized by low levels of pollution, while the fourth cluster primarily

Table 4: Values of geochemical ratios based on alkyl aromatic hydrocarbons for soil extracts

Sample code	MNR [1]	MPI-3 [2]	MPI-1 [3]	R_c [4]	Sample code	MNR [1]	MPI-3 [2]	MPI-1 [3]	R_c [4]
BS1I	-	1.59	2.38	1.83	BS1II	2.23	1.47	2.20	2.38
BS2I	1.41	1.41	2.12	2.31	BS2II	2.57	1.48	2.22	2.40
BS3I	1.72	1.42	2.13	2.32	BS3II	1.73	1.74	2.60	2.74
BS4I	1.50	1.63	2.44	2.60	BS4II	1.50	1.82	2.73	2.85
BS5I	-	1.16	1.74	1.96	BS5II	1.64	1.40	2.10	2.29
BS6I	0.97	1.78	2.67	2.81	BS6II	2.51	1.72	2.57	2.72
BS7I	1.20	1.42	2.13	2.32	BS7II	2.42	1.47	2.21	2.39
BS8I	1.34	1.61	2.42	2.57	BS8II	2.51	1.24	1.86	2.08
BS9I	2.54	1.19	1.78	2.01	BS9II	2.46	1.51	2.27	2.44
BS10I	1.51	1.62	2.43	2.59	BS10II	1.20	1.94	2.92	3.03
BS11I	2.90	1.09	1.64	1.87	BS11II	2.35	1.76	2.65	2.78
BS12I	2.48	1.53	2.30	2.47	BS12II	2.51	1.46	2.19	2.37
BS13I	2.95	1.24	1.86	2.08	BS13II	2.42	1.58	2.36	2.53
BS14I	2.99	1.34	2.01	2.21	BS14II	1.83	1.68	2.52	2.66
BS15I	3.65	1.37	2.06	2.25	BS15II	2.41	1.60	2.40	2.56
V. r.	0.00-3.65	1.09-1.78	1.64-2.67	1.83-2.60	V. r.	1.20-2.57	1.24-1.94	1.86-2.92	2.08-3.03
Av.	2.09	1.43	2.14	2.28	Av.	2.15	1.59	2.39	2.55
S. d.	0.86	0.20	0.30	0.29	S. d.	0.45	0.18	0.28	0.25

includes areas with a reduced risk of pollution. Differences between the two measurement series for some locations result primarily from environmental variability, as observed for sample BS11, or from variations in traffic intensity across different periods of the year, as in the case of sample BS6. Variability in cluster membership over time warrants particular attention in the context of future monitoring of PAH content in soils for these areas.

Statistical interpretation of results

In general, all environmental toxicity indicators show substantially higher values for the autumn samples (series II), with $\sum PAH_{carc}/\sum PAH$ being the only exception. This subset also exhibits a much wider range of values which is reflected in the standard deviation and error values (Table 3). Since the autumn samples were collected in November, i.e., well within the heating season in Poland, low emissions from domestic sources are most likely responsible for such a trend. This source of contamination is highly variable, depending on combustion conditions such as furnace type, age, and oxygen availability in the combustion zone. This affect PAHs distribution and concentration levels leading to higher variability of the toxicity indicators. In contrast, for the late spring samples, traffic is the predominant source. Improvements in combustion efficiency and flue gas filtration implemented in recent years have led to higher uniformity of the PAHs emission due to more comparable combustion parameters.

The average percentage contents of 2-, 3-, 4-, 5-, and 6-ring PAHs in the investigated soil are very similar in the both soil subsets. The autumn samples (series II) are richer in 3-ring PAHs compared to the late spring samples, which are richer in 4-ring PAHs. The other PAH groups show comparable average contents. The values of standard deviation and errors are also similar for both samples subsets. Standard deviation is highest for the most abundant PAHs, i.e. 3- and 4- ring compounds, and lowest for the lightest (2-ring) and heaviest (6-ring) PAHs.

For geochemical ratios based on alkyl aromatic hydrocarbons, the values of standard deviation and errors are similar in both sample subsets (Table 4). The highest standard deviation values are observed for the MNR index, reaching 0.86 in early spring samples and 0.45 in late autumn samples.

Changes concentrations in soil

Soil sampling locations were classified according to their site characteristics, taking into account potential pollution sources, negative external factors and frequency of attendance. Six different groups were distinguished:

- (I) BS1, BS2 – areas of power plants and combined heat and power plants; potential pollution originates from plant operations and nearby traffic**.**
- (II) BS7, BS9, BS15 – road intersections and streets with high traffic intensity; potential pollution is associated with vehicle exhaust emissions.
- (III) BS3, BS6, BS10, BS11, BS12, BS14 – areas with high population density (residential estates, schools, commercial buildings); potential contamination arises from residential heating and urban traffic**.**
- (IV) BS5 – an area of single-family housing adjacent to a forest; potential pollution sources include domestic heating (e.g., fireplaces) and nearby traffic.
- (V) BS4, BS8 –arable land and tree cover; potential contamination is related to agricultural machinery and human activity.
- (VI) BS13 – an industrial area; potential contamination originates from a nearby concrete production plant.

In the power plant areas (group I), overall PAH concentrations were lower in autumn than in late spring. This suggests that these infrastructures are well-managed, as higher PAH concentrations in such areas are typically observed in autumn/winter (You et al. 2024). However, concentrations of the heaviest 5- and 6-ring PAHs increased by more than twofold, which may indicate intensified activity in these sites since autumn. Elevated PAH concentrations during warmer periods may also result from increased road traffic and atmospheric conditions (Zhu et al. 2024).

In group II, associated with high traffic areas, PAH concentrations were higher in May than in November. The first period coincides with increased road traffic, which also contributed to fourfold higher concentrations of 5- and 6-ring PAHs, which are considered as indicators of vehicle emissions (Tian et al. 2013). Concentrations of 2-ring naphthalene did not change significantly.

In group III, representing high-population-density areas (residences and public spaces), changes in PAH pollution varied. Three out of four housing estates sampled (BS10, BS12, BS14) and the city center site (BS3) showed higher PAH concentrations in late autumn, with 3- and 4-ring PAHs increasing on average threefold. In contrast, sample BS6, collected near a public school, recorded increases in May. These differences likely reflect local factors such as traffic patterns and urban development.

Allotment gardens (group IV) showed higher PAH concentrations in November, likely due to heating in domestic fireplaces and stoves, which is consistent with previous studies (Lia et al. 2024). This was reflected in increases in 5- and 6-ring PAHs by 15% and 100%, respectively. Naphthalene concentrations also rose significantly, from 0.49 to 6.52 μg/g).

In group (V), areas located away from urban development, PAH concentrations were generally higher in November. Samples from agricultural fields showed only minor seasonal changes, suggesting limited influence from external pollutant sources, likely only agricultural machinery. However, the BS4 sample showed a greater increase in PAH concentrations, possibly reflecting increased human activity in this area during that period.

Finally, in group VI, the industrial plant area, PAH concentrations were also higher in late autumn. This increase likely reflects intensified plant operations, with average PAH concentrations approximately doubling.

Diagnostic indicators of PAHs and sources of contamination

PAH diagnostic coefficients are widely used in scientific studies to identify potential sources of PAH pollution (Rajeev et al. 2023, Yunker et al. 2002). Such sources may include the combustion of fossil fuels, wood, road traffic, urban emissions (Cieślik and Fabiańska 2021), or ecological events such as fires (Rykała et al. 2024). Various types of PAH diagnostic indicators were used to assess and identify the possible contamination sources in the study area (Table 5 and Figure

6), including: (i) fluoranthene and pyrene, (ii) anthracene and phenanthrene, (iii) benzo(a)anthracene and chrysene, and (iv) indeno[1,2,3-cd]pyrene and benzo(g,h,i)perylene.

Soil samples collected during both sampling periods fall within the biomass and hard coal combustion range, indicating the influence of combustion-related sources. Firstly, strong emitters such as hard coal or its derivatives are present in the areas where the samples were collected. Secondly, the city of Będzin, part of the Zagłębie Dąbrowskie region, has a long history of pollution from external sources (Kozielska and Rogula-Kozłowska et al. 2014), including numerous hard coal mines, industrial plants, and metallurgical facilities, which have contributed to the contamination of the natural environment.

The diagnostic results and PAH concentrations in the tested soil samples from Będzin show the legacy of these past pollutant sources (mines, industry, transport) consistent with observations from nearby cities (Dąbrowa Górnicza, Katowice, Sosnowiec, and Bytom) (Moździerz et al. 2011, Rykała et al. 2024). The residual effects of past industrial and anthropogenic activities are still evident in the analyzed soil samples, likely due to the substantial accumulation of both organic and inorganic compounds, which may have influenced the observed test results (Fabiańska et al. 2015). Spatial clustering of soil samples from both sampling periods (Figure 6), suggests consistent contamination patterns over time, implying that the same sources continue to influence these sites. Consequently, seasonal variation appears not have minimal impact on the type of potential pollution sources in the studied areas.

The BaP/(BaP+Ch) ration ranged from 0.17 to0.35, indicating contributions primarily from motor vehicles emissions (Pokhrel et al. 2018) and diesel fuel combustion (Laraa et al. 2022). This pattern is particularly evident in high-traffic sites BS7, BS9, BS15, with higher ratios observed in May, consistent with increased vehicular activity. Samples

Table 5: Values of diagnostic PAH ratios

Sample code	P/A	A/P	A/(A+P)	Fl/ (Fl+Py)	Fl/Py	Fl/ (Fl+P)	BaA/ (BaA + Ch)	BaP/ BghiP	IP/ BghiP	IP/(IP + BghiP)	BaA/ BaP	BaP/ (BaP + Ch)
BS1I	6.13	0.16	0.14	0.55	1.20	0.70	0.41	-	-	-	2.98	0.19
BS2I	2.60	0.38	0.28	0.56	1.26	0.75	0.48	10.33	1.65	0.62	4.11	0.18
BS3I	6.07	0.16	0.14	0.54	1.16	0.75	0.42	2.83	1.04	0.51	1.73	0.30
BS4I	6.14	0.16	0.14	0.56	1.30	0.58	0.41	-	-	-	3.49	0.17
BS5I	5.33	0.19	0.16	0.53	1.12	0.75	0.40	-	-	-	2.23	0.23
BS6I	9.87	0.10	0.09	0.57	1.31	0.57	0.44	2.92	1.11	0.53	2.56	0.24
BS7I	4.66	0.21	0.18	0.55	1.23	0.70	0.44	2.83	1.04	0.51	1.85	0.30
BS8I	2.94	0.34	0.25	0.54	1.18	0.72	0.47	2.75	1.02	0.50	1.78	0.33
BS9I	3.81	0.26	0.21	0.54	1.19	0.83	0.50	2.22	1.04	0.51	1.92	0.35
BS10I	5.40	0.19	0.16	0.55	1.24	0.67	0.47	2.92	1.05	0.51	2.07	0.30
BS11I	3.53	0.28	0.22	0.52	1.09	0.79	0.39	3.50	1.02	0.50	1.67	0.27
BS12I	5.00	0.20	0.17	0.55	1.21	0.66	0.42	4.75	1.04	0.51	2.54	0.22
BS13I	4.87	0.21	0.17	0.54	1.16	0.74	0.38	-	-	-	2.20	0.22
BS14I	5.57	0.18	0.15	0.55	1.22	0.71	0.42	3.76	1.09	0.52	2.20	0.25
BS15I	4.59	0.22	0.18	0.52	1.09	0.74	0.43	3.86	1.03	0.51	2.18	0.26
V. r.	2.60-9.87	0.10-0.38	0.09-0.28	0.52-0.57	1.09-1.31	0.67-0.83	0.38-0.50	0.00-10.33	0.00-1.65	0.00-0.62	1.67-4.11	0.17-0.35
Av.	5.10	0.22	0.18	0.54	1.20	0.71	0.43	3.88	1.10	0.52	2.37	0.25
S. d.	1.73	0.07	0.05	0.01	0.07	0.07	0.03	2.25	0.18	0.03	0.69	0.05
BS1II	5.54	0.18	0.15	0.54	1.19	0.71	0.46	3.17	1.11	0.53	2.55	0.25
BS2II	7.00	0.14	0.12	0.54	1.18	0.72	0.43	4.87	1.28	0.56	2.17	0.26
BS3II	5.08	0.20	0.16	0.56	1.27	0.61	0.48	3.83	1.19	0.54	2.89	0.24
BS4II	8.87	0.11	0.10	0.57	1.34	0.54	0.48	2.89	1.20	0.55	2.26	0.29
BS5II	3.65	0.27	0.21	0.56	1.30	0.59	0.41	1.60	0.96	0.49	3.50	0.17
BS6II	8.08	0.12	0.11	0.55	1.24	0.70	0.47	3.86	1.27	0.56	2.71	0.24
BS7II	6.43	0.16	0.13	0.53	1.14	0.75	0.44	4.08	1.27	0.56	2.21	0.26
BS8II	5.82	0.17	0.15	0.54	1.20	0.68	0.46	3.21	1.13	0.53	3.40	0.20
BS9II	7.07	0.14	0.12	0.54	1.20	0.70	0.45	5.01	1.24	0.55	2.81	0.23
BS10II	2.93	0.34	0.25	0.54	1.20	0.56	0.55	3.36	1.33	0.57	2.05	0.37
BS11II	4.35	0.23	0.19	0.55	1.25	0.65	0.49	3.81	1.21	0.55	3.06	0.24
BS12II	4.62	0.22	0.18	0.54	1.16	0.67	0.44	3.08	1.14	0.53	1.91	0.29
BS13II	4.27	0.23	0.19	0.54	1.18	0.68	0.45	4.59	1.28	0.56	2.79	0.23
BS14II	4.32	0.23	0.19	0.56	1.29	0.54	0.49	3.02	1.12	0.53	3.21	0.23
BS15II	4.63	0.22	0.18	0.55	1.20	0.66	0.47	3.56	1.18	0.54	3.56	0.20
V. r.	2.93-8.87	0.11-0.34	0.10-0.25	0.53-0.57	1.16-1.34	0.54-0.75	0.41-0.55	1.60-5.01	0.96-1.33	0.49-0.57	1.91-3.56	0.17-0.37
Av.	5.51	0.20	0.16	0.55	1.22	0.65	0.46	3.60	1.19	0.54	2.74	0.25
S. d.	1.68	0.06	0.04	0.01	0.06	0.07	0.03	0.87	0.09	0.02	0.54	0.05

P - phenanthrene, A - anthracene, Fl - fluoranthene, Py - pyrene, BaA - benzo(a)anthracene, Ch - chrysene, BaP - benzo(a)pyrene, BeP - benzo(e)pyrene, Pe - perylene, IP - indeno(1,2,3-cd)pyrene, BghiP - benzo(ghi)perylene, "–" Compounds not found or present but in concentrations too low to calculate a parameter value, V. r. – Values range, Av. – Average values, S. d. - Standard deviation.

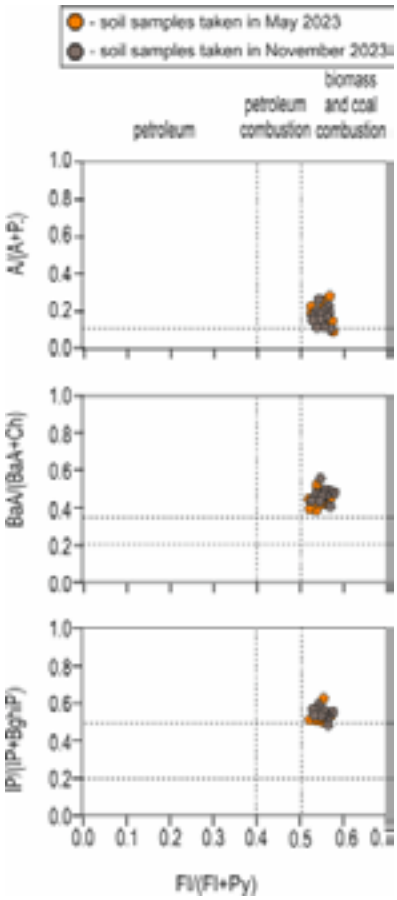

Fig. 6. Diagnostic diagrams of PAHs for soil samples. A - anthracene, P - phenanthrene, Fl - fluoranthene, Py - pyrene, BaA - benzo(a)anthracene, Ch - chrysene, IP – indeno[1,2,3-cd]pyrene, BghiP - benzo(ghi)perylene

from power plant areas (BS1, BS2) also exhibited elevated BaP/(BaP+Ch) ratios in May. The A/(A + P) ratio exceeded 0.1 in virtually all samples, indicating combustion as a dominant source of pollution, with slightly higher values in late autumn. The BaA/(BaA + Ch) ratio, greater then 0.35 in all samples, may indicate pyrogenic conditions. The IP/(IP+BghiP) ratio >0.5 suggests contributions from coal and wood combustion, indicating long-term industrial pollution. The Fl/(Fl + Py) ratio was consistent across samples (0.52-0.57), reflecting uniform contributions from urban atmospheric sources (Yunker et al. 2002) . Additionally, the fluoranthene-to-pyrene ratio (Fl/Py) exceeded 1 in all samples, conforming the pyrogenic origin of the PAHs (Rajeev et al. 2023).

The results from soil samples collected in the city of Będzin confirm significant accumulation of PAHs, reflecting the long-term impact of sources such as road traffic and urban industry. The IP/(IP+BghiP) ratio, representing the heaviest 6-ring PAHs, indicates a sustained contribution from industrial activities. These PAHs are strongly retained in the soil and persist for many years, despite leaching by rainfall. Additionally, 4-ring PAHs, specifically BaA and Ch, indicate substantial contribution from road transport (Tanić et al. 2023), which is evident in the tested samples.

In addition to the methods used to assess health risks, future studies could incorporate additional indicators. One widely used measure is the Incremental Lifetime Cancer Risk (ILCR), which quantifies the increased probability of developing cancer over a lifetime due to exposure to a specific carcinogen. An ILCR value below one in a million (10^{-6}) is typically considered an acceptable or negligible. Non-carcinogenic health effects can be evaluated using the Hazard Quotient (HQ) and Hazard Index (HI). The HQ is calculated by comparing the estimated exposure dose of a substance to its Reference Dose (RfD), a level deemed safe for chronic exposure. HQ values below one indicate that adverse non-carcinogenic health effects are unlikely. Another important indicator is the Loss of Life Expectancy (LLE), which estimates the average reduction in life expectancy expressed in days, months, or years, for a population exposed to pollution. This metric is particularly useful for conveying the societal burden of environmental contamination.

Conclusions

Soils contaminated with polycyclic aromatic hydrocarbons (PAHs) represent a significant environmental concern, particularly in urban riverine areas affected by intensive mining and industrial activities. This study investigates the seasonal variability and potential sources of PAH contamination in the eastern region of Będzin, southern Poland. The results indicate that both site-specific characteristics and sampling season exert a notable influence on PAH concentrations in soils. Areas in proximity to heavy traffic corridors and power plants exhibited elevated PAH levels in late spring, whereas residential zones with high population density showed higher concentrations in late autumn. Despite these spatial and temporal variations, carcinogenic and mutagenic risk indices derived from PAH profiles suggest no immediate health risk to the local population.

PAH diagnostic coefficients are a well-established and effective tool for identifying potential source of pollution in a given area. Combining these coefficients with geochemical indicators based on alkyl aromatic hydrocarbons enhances the accuracy and reliability of sources of identification. The results indicate contributions from multiple sources, including vehicle traffic, domestic coal combustion, urban atmospheric emissions, and public transport. It has also been documented that substantial quantities of pollutants have accumulated over many years in soils affected by historical industrial plants and mines located in these areas.

Historical accumulation of pollutants from former industrial facilities and mines has led to persistent soil contamination in the region. Consequently, continuous and systematic monitoring of pollutant levels in urban areas, particularly in southern Poland, is essential. Future research should focus on the application of statistical approaches, including multivariate analyses and health risk indices, to provide more quantitative evidence of contamination and to evaluate potential long-term health risks to urban residents.

References

Abdel-Shafy, H. & Mansourm, M. (2016). A review on polycyclic aromatic hydrocarbons: Source, environmental impact, effect on human health and remediation, *Egyptian Journal of Petroleum*, 25, 107–123. DOI:10.1016/j.ejpe.2015.03.011

Almouallem, W., Michel, J., Dorge, S., Joyeux, C., Trouvé, G. & Le Nouen, D. (2023). A comparative study of the sorption of

Nomenclature	
A - anthracene	**Ace -** acenaphthene
Acy - acenaphthylene	**Av.** – average values
BaA - benzo(a)anthracene	**BaF -** benzo(a)fluoranthene
BaP - benzo(a)pyrene	**Bb+kF -** benzo(b+k)fluoranthene
BcPhe - benzo(c)phenanthrene	**BeP -** benzo(e)pyrene
BghiP - benzo(ghi)perylene	**Ch –** chrysene
DCM - dichloromethane	**F -** fluorene
Fl - fluoranthene	**GC-MS -** Gas chromatography-mass spectrometry
HI – the Hazard Index	**HQ** - the Hazard Quotient
ILCR - Incremental Lifetime Cancer Risk	**IP -** indeno[1,2,3-cd]pyrene
LODs - the limits of detection	**LLE -** Loss of Life Expectancy
MEF - Mutagenic Potency Factors	**MEQ -** Mutagenicity Equivalent
MNR - Methylnaphthalene Ratio	**MPI -** Methylphenanthrene Index
N - naphthalene	**P -** phenathrene
PAHs - Polycyclic aromatic hydrocarbons	**PCB -** Polychlorinated Biphenyls
Pe - perylene	**Py -** pyrene
QA - Quality Assurance	**QC -** Quality Control
R_c - Vitrinite Reflectance	**RfD** - Reference Dose
RTBaP - Toxicity Equivalent	**S. d.** - standard deviation
TEF - Toxicity Equivalence Factor	**TEQ -** Toxic Equivalent
TNR - Trimethylnaphthalene Ratio	**V. r.** – values range
$\sum PAH_{carc}/\sum PAH$ - the ratio of PAHs considered to be carcinogenic to the sum of all determined PAHs	

O-PAHs and PAHs onto soils to understand their transport in soils and groundwater, *Journal of Environmental Sciences*, 124, 61–75. DOI: 10.1016/j.jes.2021.11.001

Błaszczyk, E., Rogula-Kozłowska, W., Klejnowski, K., Fulara, I. & Mielżyńska-Švach, D. (2016). Polycyclic aromatic hydrocarbons bound to outdoor and indoor airborne particles (PM2.5) and their mutagenicity and carcinogenicity in Silesian kindergartens, Poland, *Air Quality, Atmosphere & Health*, 10, 389–400. DOI: 10.1007/s11869-016-0457-5

Bukowska, B., Mokra, K. & Michałowicz, J. (2022). Benzo[a] pyrene—Environmental Occurrence, Human Exposure, and Mechanisms of Toxicity, *International Journal of Molecular Sciences*, 23, 6348. DOI: 10.3390/ijms23116348

Cieślik, E. & Fabiańska, J.M. (2021). Preservation of geochemical markers during co-combustion of hard coal and various domestic waste materials, *Science of the Total Environment*, 768, 144638. DOI: 10.1016/j.scitotenv.2020.144638

Fabiańska, M., Kozielska, B. & Konieczyński, J. (2017). Differences in the Occurrence of Polycyclic Aromatic Hydrocarbons and Geochemical Markers in the Dust Emitted from Various Coal-Fired Boilers, *Energy & Fuels*, 31, 2585–2595. DOI: 10.1021/acs.energyfuels.6b03030

Fabiańska, M.J., Kozielska, B., Konieczyński, J. & Kowalski, A. (2015). Sources of organic pollution in particulate matter and soil of Silesian Agglomeration (Poland): evidence from geochemical markers, *Environmental Geochemistry and Health*, 38, 821-842. DOI: 10.1007/s10653-015-9764-2

Gutierrez-Urbano, I., Villen-Guzman, M., Perez-Recuerda, R. & Rodriguez-Maroto, J. (2021). Removal of polycyclic aromatic hydrocarbons (PAHs) in conventional drinking water treatment processes, *Journal of Contaminant Hydrology*, 243, 103888. DOI: 10.1016/j.jconhyd.2021.103888

Jung, K.H., Yan, B., Chillrud, S.N., Perera, F.P., Whyatt, R., Camann, D., Kinney, P.L. & Miller, R.L. (2010). Assessment of Benzo(a)pyrene-equivalent Carcinogenicity and Mutagenicity of Residential Indoor versus Outdoor Polycyclic Aromatic Hydrocarbons Exposing Young Children in New York City, *International Journal of Environmental Research and Public Health*, 7, 1889-1900. DOI: 10.3390/ijerph7051889

Kozielska, B. & Rogula-Kozłowska, W. (2014). Polycyclic aromatic hydrocarbons in particulate matter in the cities of Upper Silesia, *Archives of Waste Management and Environmental Protection*, 16, 75-84.

Laraa, S., Villanuevaa, F., Martínc, P., Salgadoc, S., Morenod, A. & Sanchez-Verdúd, P. (2022). Investigation of PAHs, nitrated PAHs and oxygenated PAHs in PM10 urban aerosols. A comprehensive data analysis, *Chemosphere*, 294, 133745. DOI: 10.1016/j.chemosphere.2022.133745

Lehndorff, E. & Schwark, L. (2004). Biomonitoring of air quality in the Cologne Conurbation using pine needles as a passive sampler—Part II: polycyclic aromatic hydrocarbons (PAH), *Atmospheric Environment*, 38, 3793–3808. DOI: 10.1016/j.atmosenv.2004.03.065

Lia, S., Liua, X., Wanga, J., Lic, J., Wanga, Z., Mae, S., Donga, Z., Lia, M., Hanb, Y. & Caob, J. (2024). Exposure to polycyclic

aromatic hydrocarbons (PAHs) from domestic heating and cooking combustion of different fuel types for elders in rural China, *Environmental Pollution*, 357124416. DOI: 10.1016/j.envpol.2024.124416

Liu, L., Chen, X., Duan, Y., Wu Z. & Xu, L. (2024). Distribution, sources and health risk assessment of polycyclic aromatic hydrocarbons in urban soils under different landform conditions of Taiyuan, China, *Frontiers in Environmental Science*, 12, 1363297. DOI: 10.3389/fenvs.2024.1363297

Lopes, T., Furlong, E. & Pritt, J. (1998). Occurrence and distribution of semivolatile organic compounds in stream bed sediments, United States, 1992–95, *In ASTM International eBooks*, pp. 105–115. DOI: 10.1520/STP12158S

Maliszewska-Kordybach, B., Smreczak, B., Klimkowicz-Pawlas, A. & Terelak, H. (2008). Monitoring of the total content of polycyclic aromatic hydrocarbons (PAHs) in arable soils in Poland, *Chemosphere*, 73, 1284–1291. DOI: 10.1016/j.chemosphere.2008.07.009

Mojiri, A., Zhou, J., Ohashi, A., Ozaki, N. & Kindaichi, T. (2019). Comprehensive review of polycyclic aromatic hydrocarbons in water sources, their effects and treatments, *Science of the Total Environment*, 696, 133971. DOI: 10.1016/j.scitotenv.2019.133971

Możdzierz, A., Juszko-Piekut, M., Stojko, J., Kołosza, K., Kaźmierczak, J. & Król, M. (2011). Benzo(a)pyrene Emissions in Cities of the Upper Silesia Industrial Area in Southern Poland: 1980-2005, *Polish Journal of Environmental Studies*, 20, 1251-1258.

Nádudvari, Á. & Fabiańska, M.J. (2015). Coal-related sources of organic contamination in sediments and water from the Bierawka River (Poland), *International Journal of Coal Geology*, 152, 94-109. DOI: 10.1016/j.coal.2015.11.006

Ncube, S., Madikizela, L., Cukrowska, E. & Chimuka, L. (2018). Recent advances in the adsorbents for isolation of polycyclic aromatic hydrocarbons (PAHs) from environmental sample solutions, *TrAC Trends in Analytical Chemistry*, 99, 101–116. DOI: 10.1016/j.trac.2017.12.007

Paradelo, R., Celeiro, M., Herbon, C., Barral, M.T. & García-Jares, C. (2023). Polycyclic aromatic hydrocarbons concentration and spatial distribution in the soils of Santiago de Compostela (northwestern Spain), *Geoderma Regional*, 34, e00703. DOI: 10.1016/j.geodrs.2023.e00703

Pokhrel, B., Gong, P., Wang, X., Wang, C. & Gao, S. (2018). Polycyclic aromatic hydrocarbons in the urban atmosphere of Nepal: distribution, sources, seasonal trends, and cancer risk, *Science of The Total Environment*, 618, 1583–1590. DOI: 10.1016/j.scitotenv.2017.09.329

Radke, M. (1988). Organic geochemistry of aromatic hydrocarbons, *Adv. Pet. Geochemistry*, 2, 141–203.

Radke, M., Welte, D.H. & Willsch, H. (1986). Maturity parameters based on aromatic hydrocarbons: Influence of the organic matter type, *Organic Geochemistry*, 10, 51–63. DOI: 10.1016/0146-6380(86)90008-2

Rajeev, P., Shukla, P.Ch., Singh, G.K., Das, D. & Gupta, T. (2023). Assessment of entrainment of key PAHs emanating from major combustion sources into the ambient air, *Fuel*, 347, 128430. DOI: 10.1016/j.fuel.2023.128430

Ramesh, A., Walker, S., Hood, D., Guillén, M., Schneider, K. & Weyand, E. Bioavailability and risk assessment of orally ingested polycyclic aromatic hydrocarbons, *International Journal of Toxicology*, 23, 301–333. DOI: 10.1080/10915810490517063

Rogula-Kozłowska, W., Kozielska, B. & Klejnowski, K. (2013). Concentration, origin and health hazard from fine particle-bound PAH at three characteristic sites in southern Poland, *Bulletin of Environmental Contamination and Toxicology*, 91, 349–355. DOI: 10.1007/s00128-013-1060-1

Rykała, W., Fabiańska, J.M., Dąbrowska, D. & Nourani, V. (2023). PAHs and organophosphorus substances in burnt landfill material as a potential source of water and soil pollution, *Geological Quarterly*, 67, 1-13. DOI: 10.7306/gq.1712

Rykała, W., Fabiańska, J.M., Dąbrowska, D. & Sołtysiak, M. (2024). Geochemical markers in the detection and identification of fossil fuels in waste material from an illegal landfill fire, *Applied Geochemistry*, 176, 106214. DOI: 10.1016/j.apgeochem.2024.106214

Shamilishvily, G., Abakumov, E. & Gabov, D. (2018). Polycyclic aromatic hydrocarbon in urban soils of an Eastern European megalopolis: distribution, source identification and cancer risk evaluation, *Solid Earth*, 9, 669–682. DOI: 10.5194/se-9-669-2018

Sun, K., Song, Y., He, F., Jing, M., Tang, J. & Liu, R. (2021). A review of human and animals exposure to polycyclic aromatic hydrocarbons: Health risk and adverse effects, photoinduced toxicity and regulating effect of microplastics, *Science of the Total Environment*, 773, 145403. DOI: 10.1016/j.scitotenv.2021.145403

Tanić, M.N., Dinić, D., Kartalović, B., Mihaljev, Z., Stupar, S., Ćujić, M. & Onjia, A. (2023). Occurrence, Source Apportionment, and Health Risk Assessment of Polycyclic Aromatic Hydrocarbons in Soil of Urban Parks in a Mid-Sized City, *Water, Air, & Soil Pollution*, 234, 484. DOI: 10.1007/s11270-023-06504-4

Tian, Y.Z., Li, W.H., Shi, G.L., Feng, Y.C. & Wang, Y.Q. (2013). Relationships between PAHs and PCBs, and quantitative source apportionment of PAHs toxicity in sediments from Fenhe reservoir and watershed, *Journal of Hazardous Materials*, 248, 89–96. DOI: 10.1016/j.jhazmat.2012.12.054

Wang, D., Wu, S., Gong, X., Ding, T., Lei, Y., Sun, J. & Shen, Z. (2023). Characterization and Risk Assessment of PM2.5-Bound Polycyclic Aromatic Hydrocarbons and Their Derivatives Emitted from a Typical Pesticide Factory in China, *Toxics*, 11, 637. DOI: 10.3390/toxics11070637

Wang, X, Yao, T, Cong, Z, Yan, X, Kang, S & Zhang, Y. (2006). Gradient distribution of persistent organic contaminants along northern slope of central-Himalayas, China, *Science of The Total Environment*, 372, 193–202. DOI: 10.1016/j.scitotenv.2006.09.008

Wilcke, W., Bandowe, B., Lueso, M., Ruppenthal, M., del Valle, H. & Oelmann, Y. (2014). Polycyclic aromatic hydrocarbons (PAHs) and their polar derivatives (oxygenated PAHs, azaarenes) in soils along a climosequence in Argentina, *Science of the Total Environment*, 473–474, 317–325. DOI: 10.1016/j.scitotenv.2013.12.037

Vane, C., Kim, A., Beriro, D., Cave, M., Knights, K., Moss-Hayes, V. & Nathanail, P. (2014). Polycyclic aromatic hydrocarbons (PAH) and polychlorinated biphenyls (PCB) in urban soils of Greater London, UK, *Applied Geochemistry*, 51, 303–314. DOI: 10.1016/j.apgeochem.2014.09.013

You, Q., Yan, K., Yuan, Z., Feng, D., Wang, H., Wu, L. & Xu, J. (2024). Polycyclic aromatic hydrocarbons (PAHs) pollution and

risk assessment of soils at contaminated sites in China over the past two decades, *Journal of Cleaner Production*, 450, 141876. DOI: 10.1016/j.jclepro.2024.141876

Yunker, M.B., Macdonald, R.W., Vingarzan, R., Mitchell, R.H., Goyette, D. & Sylvestre, S. (2002). PAHs in the Fraser River basin: a critical appraisal of PAH ratios as indicators of PAH source and composition, *Organic Geochemistry*, 33, 489–515. DOI: 10.1016/S0146-6380(02)00002-5

Zhu, R., Wei, Y., He, L., Wang, M., Hu, J., Li, Z., Lai, Y. & Su, S. (2024). Particulate matter emissions from light-duty gasoline vehicles under different ambient temperatures: Physical properties and chemical compositions, *Science of the Total Environment*, 926, 171791. DOI:10.1016/j.scitotenv.2024.171791

Zmiany stężeń wielopierścieniowych węglowodorów aromatycznych w glebie – studium przypadku miasta w południowej Polsce

Streszczenie: Wielopierścieniowe węglowodory aromatyczne (WWA) to związki organiczne uważane za rakotwórcze, teratogenne i mutagenne, migrujące do środowiska glebowo-wodnego. Celem niniejszego artykułu jest przedstawienie potencjalnych zmian stężeń WWA w badanych próbkach glebowych z miasta Będzin, położonego w południowej Polsce, w dwóch seriach pomiarowych oraz wskazanie potencjalnego źródła zanieczyszczenia. W mieście pobrano trzydzieści próbek gleby w dwóch seriach pomiarowych. Miejsca pobrań związane z dużym ruchem komunikacyjnym i elektrowniami wykazywały średnio wyższe stężenia WWA późną wiosną. Natomiast miejsca związane z dużą gęstością zaludnienia wykazują wyższe stężenia późną jesienią. Średnie stężenie analizowanych WWA (WWA suma) w 15 próbkach gleby z pierwszego poboru (A) wyniosło 151 µg/g, natomiast z drugiego poboru (B) 246 µg/g. Wartości wskaźnika toksyczności ΣPAHcarc/ΣPAH we wszystkich badanych próbkach gleby utrzymywały się poniżej 0,4. Obecne zanieczyszczenie gleby w tym regionie wskazuje na akumulację WWA z byłych zakładów przemysłowych, a nie z obecnych. Mimo to, ważne jest stałe monitorowanie stężenia tych związków, aby zapobiec migracji zanieczyszczeń do warstw wodonośnych.